AIMS Mathematics, 11(1): 1050–1070.
DOI:10.3934/math.2026046
Received: 25 October 2025
Revised: 08 December 2025
Accepted: 07 January 2026
Published: 14 January 2026

https://www.aimspress.com/journal/Math

Research article

Identification and stability analysis for inverse diffusion-wave fractional problems

Ghaziyah Alsahli[1], Mustapha Benoudi[2], Maawiya Ould Sidi[1,*], Eid Sayed Kamel[1], Ibrahim Omer Ahmed[1], MedYahya Ould-MedSalem[3] and Hamed Ould Sidi[4]

[1] Department of Mathematics, College of Science, Jouf University, Sakaka, Aljouf 72341, Saudi Arabia

[2] National School of Applied Sciences at Université Sultan Moulay Slimane Beni Mellal, Morocco

[3] FST, University of Nouakchott, Mauritania

[4] Institut Supérieur de Comptabilité et d'Administration des Entreprises-ISCAE Nouakchott, Mauritania

* **Correspondence:** Email: msidi@ju.edu.sa.

Abstract: Inverse problems for fractional diffusion-wave equations are vital in various scientific fields, but are inherently ill-posed due to the non-local and memory effects of fractional derivatives. Resolving these challenges, particularly in reconstructing multiple unknown initial values from final time data, remains a significant mathematical and computational hurdle. This work addressed this gap by establishing the well-posedness of such inverse problems involving space-time fractional operators, specifically the fractional Caputo derivative and the fractional Laplacian. We developed a stable regularization framework based on Tikhonov's method to ensure the stability and uniqueness of the solution, despite the poorly posed nature of the problem. An efficient conjugate gradient algorithm was proposed to numerically reconstruct the unknowns, with specialized techniques to handle fractional operators effectively. Numerical experiments with exact and noisy data confirmed the robustness, accuracy, and practicality of our approach, demonstrating its potential for real-world applications in modeling anomalous diffusion, heat conduction, and structural dynamics. Our results contributed both theoretical insights and computational tools for tackling complex inverse problems in fractional systems.

Keywords: fractional equation of time and space; fractional laplacian; inverse problem; regularization method; conjugate gradient method
Mathematics Subject Classification: 35R11, 35R30, 47A52, 49M41, 49N45

1. Introduction

Fractional-order operators have recently gained attention as a promising alternative for modeling various phenomena in science and engineering, and offering the ability to capture effects that traditional operators cannot. Specifically, non-local diffusion operators, such as the fractional Laplacian, have become a popular choice for modeling diffusion processes. Within a probabilistic framework, this operator can be derived as the limit of a long jump random walk. These models find applications in diverse areas, including geophysics, anomalous transport and diffusion, image denoising, phase-field modeling, porous media flow, data analysis, elasticity, and population dynamics.

The space-time fractional diffusion equation has emerged as a fundamental tool to describe anomalous diffusion [4, 12, 15]. The fractional-time derivative is employed to capture particle trapping and adhesion behaviors, while the fractional-spatial derivative accounts for long-range particle jumps. These combined effects yield a distinctive concentration profile with pronounced peaks and extended tails. Fractional-time derivatives are used to model slow diffusion processes, while the parameter s is associated with the asymptotic properties of waiting-time distributions and Lévy stable processes. Such equations have applications in diverse fields.

In recent years, attention to inverse problems formulated with fractional derivatives has continued to expand, given their practical importance in uncovering unknown parameters or sources within these models. For example, one-dimensional time-fractional diffusion equations have been studied to establish uniqueness results using eigenfunction expansions and Gel'fand-Levitan theory [23]. Other studies have focused on reconstructing spatially varying coefficients, identifying source terms, or addressing ill-posed backward problems using regularization techniques. These problems are particularly relevant in systems where fractional derivatives introduce memory effects, enabling efficient recovery of the medium's initial state. In addition, the numerical treatment of multi-term and anomalous heat conduction models has received increasing attention. A semi-analytical Trefftz collocation scheme was introduced in [9], and further extensions using boundary collocation methods for functionally graded materials were presented in [8].

Several approaches have been developed to address inverse problems in fractional diffusion equations [20, 21] such as quasi-solution methods, eigenfunction expansions, and operator equations. These methods have been used to prove the existence, uniqueness and stability of solutions, as well as to design numerical algorithms for practical applications. Despite significant progress, challenges remain in addressing problems that combine both fractional Laplacians and fractional-time derivatives. However, these studies continue to advance our understanding of fractional models and their applications in various scientific and engineering fields.

For the simultaneous reconstruction of initial values in time fractional diffusion-wave equations, several researchers have contributed significantly to understanding and solving these problems, which arise in various applications involving anomalous diffusion processes and memory effects. In [11], the authors investigate the inverse source problem for time-fractional diffusion equations, focusing on using a posteriori boundary measurements. Their study provides valuable insight into the simultaneous determination of multiple parameters in fractional diffusion equations, demonstrating the importance of boundary data to ensure the uniqueness and stability of the solutions. In [23], they study the simultaneous inversion of two initial values in time-fractional diffusion-wave equations using Cauchy boundary data. They establish uniqueness results through the Laplace transformation and analytic

continuation methods. To address the ill-posed nature of the problem, they propose a nonstationary iterative Tikhonov regularization method, which proves effective in numerical simulations for reconstructing the initial values. In another study, in [22], they focus on the simultaneous recovery of both the source term and the initial values in time-fractional diffusion equations. They develop algorithms to recover these parameters simultaneously, which is crucial for applications in complex systems where both initial conditions and source terms are unknown. Their work expands the scope of inverse problems in fractional diffusion equations and provides practical algorithms for solving them. Moreover, in [13], the investigation contributes to the theoretical foundation of inverse problems in fractional diffusion equations. They investigated the uniqueness and stability of solutions for time-fractional diffusion models, providing a rigorous mathematical framework for addressing the ill-posedness typically associated with inverse problems in this context.

Inverse source problems for fractional diffusion-wave equations are not only of theoretical interest but also arise naturally in many branches of engineering. In this section, we highlight several application areas where the reconstruction of unknown initial values plays a crucial role.

In heat conduction, fractional models provide a more accurate description of anomalous transport in heterogeneous and composite materials. Identification of initial temperature fields or heat inputs is essential in non-destructive testing, thermal management of industrial processes, and microelectronics reliability. Foundational studies on fractional models and their applications to diffusion and heat transfer can be found in [14, 18, 19].

Fractional diffusion-wave equations describe the damping and viscoelastic behavior in beams, plates, and shells. Identifying unknown initial displacements or velocities is crucial for vibration control, structural health monitoring, and aerospace applications. Theoretical results and practical implementations of fractional operators of relevance to engineering are presented in [5, 14].

Pollutant transport in aquifers and porous soils often exhibits anomalous diffusion. Fractional advection-diffusion equations provide a better description of these processes than classical models, especially when non-Fickian effects dominate. The use of fractional calculus in environmental and hydrological systems is discussed in [5, 14].

The key contributions of this study are primarily theoretical, as we address several fundamental challenges associated with the inverse problem studied. In particular, we provide a detailed analysis of Tikhonov's regularization method in the context of a model that involves two distinct fractional operators: a time-dependent Caputo derivative and a spatially nonlocal fractional Laplacian. After reformulating the inverse problem within an optimization framework, we investigate two essential questions concerning the existence, uniqueness, and stability of the minimizer. From a numerical perspective, we also face the difficulty of approximating fractional operators, which substantially increases the complexity of the computational implementation.

The main results of this work can be summarized as follows:

(1) The existence and uniqueness of the solution to the studied inverse problem are rigorously established.
(2) Stability analysis is provided, showing that the minimization problem is well posed under the chosen regularization framework.
(3) An efficient numerical scheme based on a conjugate gradient algorithm is developed to reconstruct the two initial values.
(4) The robustness of the method is validated through numerical experiments, demonstrating accurate

reconstructions even in the presence of noise.

The organization of this paper will be as follows: In Section 1, a general introduction to the problem is provided, giving an overview of the research topic. Section 2 presents preliminary results of the fractional problem, including the development of theories that explain the existence of direct and inverse solutions to the problem. Moving to Section 3, the focus shifts to studying the inverse problem using Tikhonov's classical method. This section also delves into the examination and proof of the problems related to existence, uniqueness, and stability. Section 4 outlines the identification approach for the proposed problem, describing the methodology used in the investigation. The numerical results obtained from the research are presented and discussed in Section 5, which presents the practical implications of the proposed approach. Finally, Section 6 provides the conclusions drawn from the study, summarizing the key findings.

2. Preliminary

This section introduces the key definitions required for the next section.

Definition 2.1. *[16, 19] The fractional integral of order α in the sense of Riemann-Liouville is defined by*

$$\mathrm{I}_0^{\alpha}\Psi(t) = \frac{1}{\Gamma(\alpha)}\int_0^t (t-\nu)^{\alpha-1}\Psi(\nu)d\nu. \tag{2.1}$$

Definition 2.2. *[16, 19] For all $n-1 \leq \alpha < n$ and $n \in \mathbb{N}$. The Caputo fractional derivative of order α is expressed as*

$${}^{C}\mathrm{D}_t^{\alpha}\Psi(t) = \mathrm{I}_0^{n-\alpha}\Psi^{(n)}(t) = \frac{1}{\Gamma(n-\alpha)}\int_0^t (t-\nu)^{n-1-\alpha}\Psi^{(n)}(\nu)d\nu. \tag{2.2}$$

Definition 2.3. *[16, 19] Whenever $m-1 \leq \beta < m$ with $m \in \mathbb{N}$, the Riemann-Liouville fractional derivative of order β is given by*

$${}^{RL}\mathrm{D}_t^{\beta}\Psi(x) = \frac{d}{dt}\mathrm{I}_0^{m-\beta}\Psi(t) = \frac{1}{\Gamma(m-\beta)}\frac{d^m}{dt^m}\int_0^t (t-q)^{m-1-\beta}\Psi(q)dq. \tag{2.3}$$

For $T > 0$ and $\Omega \subset \mathbb{R}^m$, we consider the following fractional system of order $\alpha \in (1,\ 2)$ in the Caputo sense defined by:

$$\begin{cases} {}^{C}D_t^{\alpha}\Theta(x,t) = -(-\Delta)^s\Theta(x,t), & (x,t) \in \Omega \times (0,T), \\ \Theta(\xi,t) = 0, & \partial\Omega \times (0,T), \\ \Theta(x,0) = \Theta_0(x),\ \dfrac{\partial\Theta}{\partial t}(x,0) = \Theta_1(x), & x \in \Omega, \end{cases} \tag{2.4}$$

where the fractional Laplacian operator of order $s \in (0,1)$ is defined as follows:

$$(-\Delta)^s\Theta(x,t) = C_{m,s}P.V\int_{\mathbb{R}^m}\frac{\Theta(x,t)-\Theta(y,t)}{|x-y|^{2s+m}}dy, \tag{2.5}$$

with $C_{m,s}$ is a normalization constant, given by

$$C_{m,s} = \frac{4^s s\Gamma(s+\frac{m}{2})}{\pi^{\frac{m}{2}}\Gamma(1-s)},$$

and "P.V." is the principal value of the integral, defined by

$$P.V \int_{\mathbb{R}^m} \frac{\Theta(x,t)-\Theta(y,t)}{|x-y|^{2s+m}}dy = \lim_{\varepsilon\to 0}\int_{\{y\in\mathbb{R}^m,\ |y-x|>\varepsilon\}} \frac{\Theta(x,t)-\Theta(y,t)}{|x-y|^{2s+m}}dy.$$

In the following, we set some basic notations and recall some definitions and theorems. Throughout this work, $L^2 = L^2(\Omega)$ denotes the classical Hilbert space with inner product $(\cdot,\cdot)$. The spaces $H_0^1(\Omega)$, $H^1(\Omega)$, and related notation represent the standard Sobolev spaces. We use $H^s(0,T)$ to indicate the fractional Sobolev space in time (Adams [1]). Especially for $s \in (0,1)$, the fractional Sobolev space $H^s(\Omega)$ is defined by

$$H^s(\Omega) = \left\{\Theta \in L^2(\Omega) : |\Theta|_{H^s(\Omega)} = \left(\int_\Omega\int_\Omega \frac{|\Theta(x)-\Theta(y)|^2}{|x-y|^{m+2s}}\,dxdy\right)^{\frac{1}{2}} < \infty\right\}.$$

Its natural norm is defined by

$$\|\Theta\|_{H^s(\Omega)} = \left(\|\Theta\|^2_{L^2(\Omega)} + |\Theta|^2_{H^s(\Omega)}\right)^{\frac{1}{2}}.$$

Moreover, we define the fractional space $\dot{H}^s(\Omega)$ of order $s \in (0,1)$ as follows:

$$\widetilde{H}^s(\Omega) := \left\{\Theta \in H^s(\mathbb{R}^m) : \text{supp}\,\Theta \subset \overline{\Omega}\right\}.$$

For the space $H^s(\Omega)$, the corresponding bilinear form is defined as follows:

$$B_s(\Theta,\ \Phi) = C_{m,s}\int\int_{(\mathbb{R}^m\times\mathbb{R}^m)\setminus(\Omega^c\times\Omega^c)} \frac{(\Theta(x)-\Theta(y))(\Phi(x)-\Phi(y))}{|x-y|^{m+2s}}\,dx\,dy,$$

where Ω^c is the complement of Ω in $\mathbb{R}^m$.

Proposition 2.1. *(see [6]). Let $\Theta,\ \Phi : \mathbb{R}^m \to \mathbb{R}$ be smooth functions; then*

$$\int_\Omega \Phi(x)(-\Delta)^s\Theta(x)dx = \frac{B_s(\Theta,\ \Phi)}{2} - \int_{\Omega^c}\Phi(x)\mathcal{N}_s\Theta(x)dx,$$

here $\mathcal{N}_s$ represents the non-local Neumann operator associated with $(-\Delta)^s$, which is defined as follows:

$$\mathcal{N}_s\Theta(x) = C_{m,s}\int_\Omega \frac{\Theta(x)-\Theta(y)}{|x-y|^{m+2s}}\,dy.$$

The relationship between the Riemann-Liouville fractional derivative and the Caputo derivative is encapsulated in the fractional integration by parts formula. This fundamental result establishes a bridge between these two Definitions, highlighting their interconnection within fractional calculus and their overall significance.

Proposition 2.2. *[2] Let $\alpha \in (1,2)$. Let Θ_1 and Θ_2 be assumed to be absolutely integrable. Hence, we get*

$$\int_0^T \Theta_2(t)\ {}^C\mathrm{D}_t^\alpha\Theta_1(t)\,dt = \int_0^T \Theta_1(t)\ {}^{RL}\mathrm{D}_t^\alpha\Theta_2(t)\,dt + \left[\Theta_1(t)\frac{\partial}{\partial t}\mathrm{I}_t^{2-\alpha}\Theta_2(t)\right]_{t=0}^{t=T} - \left[\mathrm{I}_t^{2-\alpha}\Theta_2(t)\frac{\partial\Theta_1}{\partial t}(t)\right]_{t=0}^{t=T}.$$

Definition 2.4. *[10] A collection of bounded linear operators $\{C(t)\}_{t\in\mathbb{R}}$ on the Hilbert space $H^s(\Omega)$ is referred to as a strongly continuous cosine family if it satisfies the following conditions: $C(0) = I$, $C(s+t) + C(s-t) = 2C(s)C(t)$ for all $s, t \in \mathbb{R}$, and the map $t \mapsto C(t)\Theta$ is strongly continuous for every $\Theta \in H^s(\Omega)$.*

Let $\{S(t)\}_{t\in\mathbb{R}}$ represent the strongly continuous sine families that are related to the strongly continuous cosine families $\{C(t)\}_{t\in\mathbb{R}}$, where

$$S(t)\Theta = \int_0^t C(s)\Theta\, ds, \quad \Theta \in H^s(\Omega),\ t \in \mathbb{R}.$$

Furthermore, the operator $A = (-\Delta)^s$ is referred to as the infinitesimal generator of cosine families $\{C(t)\}_{t\in\mathbb{R}}$ if

$$A\Theta = \frac{d^2}{dt^2}C(t)\Theta\Big|_{t=0}, \quad \text{for all } \Theta \in \mathcal{D}(A),$$

the domain A is given by $\mathcal{D}(A) = \{\Theta \in H^s(\Omega) : C(t)\Theta \in C^2(\mathbb{R},\ H^s(\Omega))\}$.

Definition 2.5. *[10] We say that $\Theta \in C((0,T); H^s(\Omega)) \cap C^1([0,T]; L^2(\Omega))$ is a mild solution to Eq* (2.4) *if we have $\Theta(0) = \Theta_0$ and $\frac{\partial\Theta}{\partial t}(0) = \Theta_1$, and if*

$$\Theta(x,t) = S_\alpha(t)\Theta_0(x) + P_\alpha(t)\Theta_1(x), \tag{2.6}$$

where

$$S_\alpha(t) = \int_0^\infty M_\alpha(\theta)C(t^\alpha\theta)\, d\theta, \quad P_\alpha(t) = \int_0^t S_\alpha(s)\, ds.$$

The $M_\alpha(\theta)$ function is given by

$$M_\alpha(\theta) = \frac{1}{\alpha}\theta^{-\alpha-1}\Psi_\alpha\left(\theta^{-\frac{1}{\alpha}}\right), \quad \Psi_\alpha(\theta) = \frac{1}{\pi}\sum_{n=1}^{\infty}(-1)^{n-1}\theta^{-n\alpha-1}\frac{\Gamma(n\alpha+1)}{n!}\sin(n\pi\alpha),$$

for $\theta \in (0,\infty)$, where $M_\alpha(\cdot)$ is the Mainardi Wright-type function on $(0,\infty)$ that

$$M_\alpha(\theta) \geq 0 \quad \textit{and} \quad \int_0^\infty M_\alpha(\theta)\, d\theta = 1.$$

Remark 2.1. *The fractional Laplacian $(-\Delta)^s$ possesses a complete set of (φ_n) with associated (λ_n). Thus, the mild solution of system* (2.4) *takes the form:*

$$\Theta(x,t) = \sum_{n=0}^{+\infty}\left[E_{\alpha,1}(-\lambda_n t^\alpha)\langle\Theta_0,\ \varphi_n\rangle + tE_{\alpha,2}\left(-\lambda_n t^\alpha\right)\langle\Theta_1,\ \varphi_n\rangle\right]\varphi_n, \tag{2.7}$$

where $E_{\alpha,\beta}(z) = \sum_{n=0}^{+\infty}\frac{z^n}{\Gamma(\beta+n\alpha)}$ the Mittag-Leffl function.

The representation of the solution of the direct problem (2.4) can be derived from the following findings of this family of functions.

Lemma 2.1. *[10] Let $\alpha > 0$ and $\lambda > 0$, then we have*

$$^{C}\mathrm{D}_{t}^{\alpha} E_{\alpha,1}(-\lambda t^{\alpha}) = -\lambda E_{\alpha,1}(-\lambda t^{\alpha}), \quad t > 0. \tag{2.8}$$

Moreover, the following identity holds for integer-order differentiation:

$$\frac{d}{dt} E_{\alpha,1}(-\lambda t^{\alpha}) = -\lambda t^{\alpha-1} E_{\alpha,\alpha}(-\lambda t^{\alpha}), \quad t > 0. \tag{2.9}$$

Lemma 2.2. *[14, p. 40–45] Let $1 < \alpha < 2$. Then there exists a constant $C_0 = C_0(\alpha) > 0$ such that*

$$|E_{\alpha,1}(z)| \leq \frac{C_0}{1+|z|}, \quad |\arg(z)| \leq \pi. \tag{2.10}$$

We now verify that problem (2.4) has a unique solution.

Theorem 2.1. *Let Θ and Π be the solutions of problem* (2.4). *If $\Theta(x,T) = \Pi(x,T)$ for $x \in \Omega$ for $x \in \Omega$, then it follows that $\Theta_1 = \Pi_1$ and $\Theta_2 = \Pi_2$ in Ω.*

Proof. Using the series representations of the solutions Θ and Π, we can write

$$\Theta(x,T) = \sum_{n=0}^{+\infty} \left[E_{\alpha,1}(-\lambda_n T^{\alpha}) \langle \Theta_0,\ \varphi_n \rangle + T E_{\alpha,2}\left(-\lambda_n T^{\alpha}\right) \langle \Theta_1,\ \varphi_n \rangle \right] \varphi_n, \tag{2.11}$$

and

$$\Pi(x,T) = \sum_{n=0}^{+\infty} \left[E_{\alpha,1}(-\lambda_n T^{\alpha}) \langle \Pi_0,\ \varphi_n \rangle + T E_{\alpha,2}\left(-\lambda_n T^{\alpha}\right) \langle \Pi_1,\ \varphi_n \rangle \right] \varphi_n. \tag{2.12}$$

Since $\Theta(\cdot,T) = \Pi(\cdot,T)$ in Ω, we deduce that

$$\begin{aligned} &\sum_{n=0}^{+\infty} \left[E_{\alpha,1}(-\lambda_n T^{\alpha}) \langle \Pi_0,\ \varphi_n \rangle + T E_{\alpha,2}\left(-\lambda_n T^{\alpha}\right) \langle \Pi_1,\ \varphi_n \rangle \right] \varphi_n \\ =&\sum_{n=0}^{+\infty} \left[E_{\alpha,1}(-\lambda_n T^{\alpha}) \langle \Theta_0,\ \varphi_n \rangle + T E_{\alpha,2}\left(-\lambda_n T^{\alpha}\right) \langle \Theta_1,\ \varphi_n \rangle \right] \varphi_n. \end{aligned}$$

Based on the proof of Theorem 3.1 (see [23]), we proceed by multiplying both sides of the given equation by $\varphi_n(x)$ and then integrating the resulting expression over x. Noting that $\varphi_n = 0$ in Ω^c, we obtain

$$\begin{cases} E_{\alpha,1}(-\lambda_n T^{\alpha}) \langle \Pi_0,\ \varphi_n \rangle = E_{\alpha,1}(-\lambda_n T^{\alpha}) \langle \Theta_0,\ \varphi_n \rangle, \\ E_{\alpha,2}\left(-\lambda_n T^{\alpha}\right) \langle \Pi_1,\ \varphi_n \rangle = E_{\alpha,2}\left(-\lambda_n T^{\alpha}\right) \langle \Theta_1,\ \varphi_n \rangle, \end{cases} \quad \forall\ n \geq 0.$$

It follows:

$$\begin{cases} E_{\alpha,1}(-\lambda_n T^{\alpha}) \langle \Pi_0 - \Theta_0,\ \varphi_n \rangle = 0, \\ E_{\alpha,2}\left(-\lambda_n T^{\alpha}\right) \langle \Pi_1, \Theta_1,\ \varphi_n \rangle = 0, \end{cases} \quad \forall\ n \geq 0.$$

We know that $E_{\alpha,1}(-\lambda_n T^{\alpha}) > 0$ and $E_{\alpha,2}(-\lambda_n T^{\alpha}) > 0$. Then, we get

$$\begin{cases} \langle \Pi_0,\ \varphi_n \rangle = \langle \Theta_0,\ \varphi_n \rangle, \\ \langle \Pi_1,\ \varphi_n \rangle = \langle \Theta_1,\ \varphi_n \rangle, \end{cases} \quad \forall\ n \geq 0.$$

Implies that $\Theta_0 = \Pi_0$ and $\Theta_1 = \Pi_1$. Thus the proof is complete. □

3. Considered inverse problem

This section focuses on the mathematical examination of the inverse issue associated with the fractional hyperbolic equation of space-time (2.4). Theoretical conclusions are presented on the existence and uniqueness of solutions. First, a minimization problem is created from the inverse problem.

Consider the operator Λ defined by

$$\begin{array}{rccl} \Lambda & : & H_0^s(\Omega) \times L^2(\Omega) & \to & L^2(\Omega), \\ & & (\Theta_0,\ \Theta_1) & \mapsto & \Theta(x, T). \end{array} \tag{3.1}$$

Next, we prove that the operator Λ is compact.

Proposition 3.1. *The linear operator Λ defined by Eq* (3.1) *is a compact operator from $H_0^s(\Omega) \times L^2(\Omega)$ to $L^2(\Omega)$.*

Proof. By Eqs (2.7) and (3.1), we deduce that, for all $(\Theta_0,\ \Theta_1) \in H_0^s(\Omega) \times L^2(\Omega)$

$$\Lambda(\Theta_0,\ \Theta_1) = \sum_{n=0}^{+\infty} \left[E_{\alpha,1}(-\lambda_n T^\alpha) \langle \Theta_0,\ \varphi_n \rangle + T E_{\alpha,2}\left(-\lambda_n T^\alpha\right) \langle \Theta_1,\ \varphi_n \rangle \right] \varphi_n. \tag{3.2}$$

We define the finite rank operators Λ_N as follows:

$$\Lambda_N(\Theta_0,\ \Theta_1) := \sum_{n=0}^{N} \left[E_{\alpha,1}(-\lambda_n T^\alpha) \langle \Theta_0,\ \varphi_n \rangle + T E_{\alpha,2}\left(-\lambda_n T^\alpha\right) \langle \Theta_1,\ \varphi_n \rangle \right] \varphi_n. \tag{3.3}$$

From Eqs (3.2) and (3.3), we get

$$\|\Lambda(\Theta_0,\ \Theta_1) - \Lambda_N(\Theta_0,\ \Theta_1)\|^2_{L^2(\Omega)} \leq \sum_{k=N+1}^{+\infty} \left[\left| E_{\alpha,1}(-\lambda_k T^\alpha) \right|^2 |\langle \Theta_0,\ \varphi_n \rangle|^2 + T^2 \left| E_{\alpha,2}(-\lambda_k T^\alpha) \right|^2 |\langle \Theta_1,\ \varphi_n \rangle|^2 \right].$$

Thanks to Lemma 2.2, we obtain

$$\|\Lambda(\Theta_0,\ \Theta_1) - \Lambda_N(\Theta_0,\ \Theta_1)\|_{L^2(\Omega)} \leq \frac{C_0}{T^\alpha \lambda_N} \|\Theta_0\|_{H_0^s(\Omega)} + \frac{C_0}{T^{2\alpha-2} \lambda_N^2} \|\Theta_1\|_{L^2(\Omega)}.$$

Therefore, $\|\Lambda(\Theta_0,\ \Theta_1) - \Lambda_N(\Theta_0,\ \Theta_1))\|_{L^2(\Omega)} \to 0$ in the sense of operator norm in $L(H_0^s(\Omega) \times L^2(\Omega);\ L^2(\Omega))$ as $N \to \infty$, which completes the proof. □

To address the regularization of well-posed problems, we utilize one of the most widely applied techniques: the Tikhonov regularization method. The Tikhonov regularization functional is defined as follows:

$$(IP) \left\{ \begin{array}{l} \text{Find } \Theta_0^* \in H_0^s(\Omega) \text{ and } \Theta_1^* \in L^2(\Omega) \text{ such that} \\ Q(\Theta_0^*,\ \Theta_1^*) = \min\limits_{(\Theta_0,\ \Theta_1) \in H_0^s(\Omega) \times L^2(\Omega)} \dfrac{1}{2} \left\{ \begin{array}{l} \|\Lambda(\Theta_0,\ \Theta_1) - \Theta_{obs}\|^2_{L^2(\Omega))} \\ +\eta \left(\|\Theta_0\|^2_{H_0^s(\Omega)} + \|\Theta_1\|^2_{L^2(\Omega)} \right) \end{array} \right\}, \end{array} \right. \tag{3.4}$$

with η the Tikhonov regularization parameter and Θ_{obs} representing the observer conditions.

In the next step, we will examine this minimization problem and discuss the existence, uniqueness, and stability issues.

Proposition 3.2. *The function Q has a finite infinitum on $L^2(\Omega)$, i.e.,*

$$\min_{(\Theta_0,\ \Theta_1)\in H_0^s(\Omega)\times L^2(\Omega)} Q(\Theta_0,\ \Theta_1) \ \text{ is finite.} \tag{3.5}$$

Moreover, there exists $(\Theta_0,\ \Theta_1)^* \in H_0^s(\Omega)\times L^2(\Omega)$ a sequence $\{(\Theta_0,\ \Theta_1)^n\}_{n\geq 1} \subset H_0^s(\Omega)\times L^2(\Omega)$, such that

$$(\Theta_0,\ \Theta_1)^n \rightharpoonup (\Theta_0,\ \Theta_1)^* \quad in \quad H_0^s(\Omega)\times L^2(\Omega) \quad as \quad n\to\infty,$$

where "$\rightharpoonup$" denotes the weak convergence symbol.

Proof. The functional Q is constructed to be non-negative. Applying Lemma 3.1 (see [3]), there exists a minimizing sequence $\{(\Theta_0,\ \Theta_1)^n\}_{n\geq 1}$ in $H_0^s(\Omega)\times L^2(\Omega)$ such that

$$\lim_{n\to\infty} Q((\Theta_0,\ \Theta_1)^n) = \min_{(\Theta_0,\ \Theta_1)\in H_0^s(\Omega)\times L^2(\Omega)} Q(\Theta_0,\ \Theta_1).$$

Using the relation (25) (see [3]), we deduce:

$$0 \leq Q((\Theta_0,\ \Theta_1)^n) \leq Q(0) + c = \|\Theta_{obs}\|_{L^2(\Omega)} + c,$$

where $c \geq 1$ is an arbitrary constant.

As a result, there exists a constant $B > 0$ such that

$$\|(\Theta_0,\ \Theta_1)^n\|_{H_0^s(\Omega)\times L^2(\Omega)} \leq B, \quad \forall n \in \mathbb{N}^*.$$

This implies that the sequence $\{(\Theta_0,\ \Theta_1)^n\}_{n\geq 1}$ is uniformly bounded in $H_0^s(\Omega)\times L^2(\Omega)$. Consequently, there exist an element $(\Theta_0,\ \Theta_1)^* \in H^1(\Omega)\times L^2(\Omega)$ and a subsequence of $\{(\Theta_0,\ \Theta_1)^n\}_{n\geq 1}$, still denoted by $\{(\Theta_0,\ \Theta_1)^n\}_{n\geq 1}$, such that

$$(\Theta_0,\ \Theta_1)^n \rightharpoonup (\Theta_0,\ \Theta_1)^* \quad \text{in } H_0^s(\Omega)\times L^2(\Omega) \quad \text{as } n\to\infty.$$

□

Theorem 3.1. *Let $\Theta_{obs} \in L^2(\Omega)$ be an observed data set measured in a specific domain Ω. Then, the minimization problem (IP) possesses a unique solution $(\Theta_0,\ \Theta_1)^* = (\Theta_0^*,\ \Theta_1^*) \in H_0^s(\Omega)\times L^2(\Omega)$, such that*

$$Q(\Theta_0^*,\ \Theta_1^*) \leq Q(\Theta_0,\ \Theta_1), \quad \forall (\Theta_0,\ \Theta_1) \in H_0^s(\Omega)\times L^2(\Omega). \tag{3.6}$$

Proof. According to Proposition 3.2 and due to the non-negativity of the function Q, there exists a uniformly bounded sequence $\{(\Theta_0,\ \Theta_1)^n\}_{n\geq 1} \subset H_0^s(\Omega)\times L^2(\Omega)$. This ensures the existence of an element $(\Theta_{0*},\ \Theta_1^*) \in H_0^s(\Omega)\times L^2(\Omega)$ and a subsequence of $\{(\Theta_0,\ \Theta_1)^n\}_{n\geq 1}$, which we continue to denote by $\{(\Theta_0,\ \Theta_1)^n\}_{n\geq 1}$, such that

$$(\Theta_0,\ \Theta_1)^n \rightharpoonup (\Theta_0,\ \Theta_1)^* \quad \text{in } H_0^s(\Omega)\times L^2(\Omega), \quad \text{as } n\to\infty.$$

From Proposition 3.4 (see [3]), it follows that:

$$Q((\Theta_0,\ \Theta_1)^*) \leq \liminf_{n\to\infty} Q((\Theta_0,\ \Theta_1)^n) = \inf_{(\Theta_0,\ \Theta_1)H_0^s(\Omega)\times\in L^2(\Omega)} Q(\Theta_0,\ \Theta_1).$$

□

4. Numerical reconstruction approach

This section is devoted to the numerical reconstruction approach for solving the minimization problem. The proposed approach is based on the derivation of an optimality condition and the conjugate gradient algorithm.

We now derive a first-order optimality condition that provides a simplified characterization of the unknown initial value $\Theta_0,\ \Theta_1$. The derivation of this condition is based on the computation of the gradient of Q, which can be obtained by constructing an adjoint problem. From now on, we denote by Θ the solution of problem (2.4) to emphasize its dependence on the unknown function $\Theta_0,\ \Theta_1$. The weak formulation of problem (2.4) is as follows: Find $\Theta \in H^{\alpha,s}(0,T;\Omega)$ such that

$$\int_0^T \int_\Omega {}^{C}D_t^\alpha \Theta \phi \, dx \, dt + \int_0^T B_s(\Theta(\cdot,t),\phi(\cdot,t))\, dt = 0, \tag{4.1}$$

for any test function $\phi \in H^s(0,T;\tilde{H}^s(\Omega) \cap H^{s+\eta}(\Omega))$ with $\mathrm{I}_t^{2-\alpha}\phi = 0$ in $\Omega \times \{T\}$.

To derive the optimality condition, we calculate the Fréshet derivative $Q'(\Theta_0,\ \Theta_1)$ of the objective functional $Q(\Theta_0,\ \Theta_1)$. By simple computations, we obtain the following:

$$\begin{aligned} Q'(\Theta_0,\ \Theta_1)\cdot(\psi_0,\ \psi_1) &= \lim_{\varepsilon\to 0} \frac{Q\left[(\Theta_0,\ \Theta_1) + \epsilon(\psi_0,\ \psi_1)\right] - Q(\Theta_0,\ \Theta_1)}{\varepsilon} \\ = \int_\Omega \left[\Theta(x,T) - \Theta_{obs}(x)\right]\psi(x,T)\, dx &+ \eta \left\langle \Theta_0(x),\ \psi_0(x)\right\rangle_{H_0^s(\Omega)} + \eta \left\langle \Theta_1(x),\ \psi_1(x)\right\rangle_{L^2(\Omega)}. \end{aligned} \tag{4.2}$$

To simplify the computational process of the Freshet derivatives, we rewrite them in their natural form. Specifically, we need to identify an explicit function $R(x)$ such that $Q'(\Theta_0,\ \Theta_1)\cdot(\psi_0,\ \psi_1) = (R,\ \psi)$. For this, we replace the term $\displaystyle\int_\Omega [\Theta(x,T) - \Theta_{obs}(x)]\,\psi(x,T)\, dx$ with a function of x.

Thus, we introduce the following adjoint problem:

$$\begin{cases} {}^{RL}D_t^\alpha \Xi = -(-\Delta)^s \Xi + [\Theta(x,T) - \Theta_{obs}(x)]\,\delta(t-T), & (x,t) \in \Omega \times (0,T], \\ \Xi = 0, & (x,t) \in \partial\Omega \times (0,T), \\ \lim\limits_{t\to T^-} \mathrm{I}_t^{2-\alpha}\Xi = \lim\limits_{t\to T^-} \dfrac{\partial}{\partial t}\mathrm{I}_t^{2-\alpha}\Xi = 0, & (x,t) \in \Omega \times \{T\}. \end{cases} \tag{4.3}$$

Here, $\delta(t-T)$ is the Dirac delta function centered on $t = T$. The weak formulation of the adjoint problem is as follows: Find $\Xi \in H^\alpha((0,T);\ \tilde{H}^s(\Omega)) \cap H^{s+\eta}(\Omega)$ such that $\mathrm{I}_t^{2-\alpha}\Xi = 0$ in $\Omega \times \{T\}$, and

$$\int_0^T \int_\Omega {}^{RL}D_t^\alpha \Xi(x,t)\psi(x,t) dx dt + \int_0^T B_s(\Xi(.,t),\ \psi(.,t))\, dt = \int_\Omega (\Theta(x,T) - \Theta_{obs}(x))\psi(x,T)\, dx, \tag{4.4}$$

for any test function $\psi \in W^{\alpha,s}(0,T;\Omega)$ with $\psi(.,0) = 0 = \dfrac{\partial \psi}{\partial t}(.,0)$ in Ω.

On the other hand, from Eq (4.1) and using integration by parts, we get the following:

$$\begin{aligned} &\int_0^T \int_\Omega \psi(x,t)\, {}^{RL}D_t^\alpha \phi(x,t)\, dx\, dt + \int_0^T B_s(\psi(\cdot,t),\ \phi(\cdot,t))\, dt \\ &= \int_\Omega \left[\frac{\partial \psi}{\partial t}(x,0)\mathrm{I}_t^{2-\alpha}\phi(x,0) - \psi(x,0)\frac{\partial}{\partial t}\mathrm{I}_t^{2-\alpha}\phi(x,0)\right] dx, \end{aligned} \tag{4.5}$$

From these considerations, we can express Ξ and ϕ as mutual test functions using identities Eqs (4.4) and (4.5). This yields

$$\int_{\Omega} [\Theta(x,T) - \Theta_{obs}(x)]\, \psi(x,T)\, dx = \int_{\Omega} \left[\psi_1(x) \mathrm{I}_t^{2-\alpha} \Xi(x,0) - \psi_0(x) \frac{\partial}{\partial t} \mathrm{I}_t^{2-\alpha} \Xi(x,0) \right] dx. \tag{4.6}$$

Thus, the Freshet derivative becomes

$$\begin{aligned} Q'(\Theta_0,\ \Theta_1) \cdot (\psi_0,\ \psi_1) = & \int_{\Omega} \left[\psi_1(x) \mathrm{I}_t^{2-\alpha} \Xi(x,0) - \psi_0(x) \frac{\partial}{\partial t} \mathrm{I}_t^{2-\alpha} \Xi(x,0) \right] dx \\ & + \eta \left\langle \Theta_0(x),\ \psi_0(x) \right\rangle_{H_0^s(\Omega)} + \eta \left\langle \Theta_1(x),\ \psi_1(x) \right\rangle_{L^2(\Omega)}. \end{aligned} \tag{4.7}$$

To minimize Q, the optimality condition is

$$\begin{cases} \mathrm{I}_t^{2-\alpha} \Xi(x,0) + \eta \Theta_1(x) = 0, \\ \dfrac{\partial}{\partial t} \mathrm{I}_t^{2-\alpha} \Xi(x,0) - \eta \Theta_0(x) = 0. \end{cases} \tag{4.8}$$

Then, the optimal solution,

$$\begin{cases} \Theta_1^*(x) = \dfrac{-1}{\eta} \mathrm{I}_t^{2-\alpha} \Xi(x,0), \\ \Theta_0^*(x) = \dfrac{1}{\eta} \dfrac{\partial}{\partial t} \mathrm{I}_t^{2-\alpha} \Xi(x,0). \end{cases} \tag{4.9}$$

The numerical algorithm that we propose is based on the conjugate gradient method and Morozov's discrepancy principle (see, e.g., [17]). Let Θ_0^k and Θ_1^k be the approximate solution of $k - th$ to Θ_0 and Θ_1. Denote

$$\begin{cases} \Theta_0^{k+1} = \Theta_0^k + \mu_k d_k^{(0)}, \\ \Theta_1^{k+1} = \Theta_1^k + \mu_k d_k^{(1)}, \end{cases} \quad k = 0, 1, ..., \tag{4.10}$$

where the initial guess Θ_0^0 and Θ_1^0 is given, the term μ_k is the step size, $d_k^{(0)}$ and $d_k^{(1)}$ are the descent directions in the kth iteration.

The conjugate gradient method uses the following iteration formula to update the descent direction. The descent direction at the k-th step is updated as follows:

$$\begin{cases} d_k^{(0)} = -\dfrac{\partial Q}{\partial \Theta_0^k}, \\ d_k^{(1)} = -\dfrac{\partial Q}{\partial \Theta_1^k}, \end{cases} \tag{4.11}$$

and for $k \geq 1$:

$$d_k^{(i)} = -\frac{\partial Q}{\partial \Theta_i^k} + \theta_k^{(i)} d_{k-1}^{(i)}, \quad i = 0, 1, \tag{4.12}$$

where

$$\theta_k^{(i)} = \frac{\| \dfrac{\partial Q}{\partial \Theta_i^k} (\Theta_0^k,\ \Theta_1^k) \|_{L^2(\Omega)}^2}{\| \dfrac{\partial Q}{\partial \Theta_i^k} (\Theta_0^{k-1},\ \Theta_1^{k-1}) \|_{L^2(\Omega)}^2}. \tag{4.13}$$

The step size μ_k is determined by minimizing

$$Q(\Theta_0^{k+1}, \Theta_1^{k+1}) = Q(\Theta_0^k + \mu_k d_k^{(0)}, \Theta_1^k + \mu_k d_k^{(1)}).$$

The condition $\dfrac{\partial Q}{\partial \mu_k} = 0$ provides an explicit formula for μ_k.

$$\mu_k = -\frac{\displaystyle\int_\Omega \left(\Lambda(\Theta_0^k, \Theta_1^k) - \Theta_{\text{obs}}\right) \Lambda(d_k^{(0)}, d_k^{(1)})\, dx + \eta\left(\langle \nabla\Theta_0^k, \nabla d_k^{(0)}\rangle_{L^2(\Omega)} + \langle \Theta_1^k,\ d_k^{(1)}\rangle_{L^2(\Omega)}\right)}{\displaystyle\int_\Omega \left|\Lambda(d_k^{(0)}, d_k^{(1)})\right|^2\ dx + \eta\left(\|d_k^{(0)}\|^2_{H^1(\Omega)} + \|d_k^{(1)}\|^2_{L^2(\Omega)}\right)}. \tag{4.14}$$

5. Numerical results

In this section, we will apply the conjugate gradient algorithm established in the previous section to the numerical treatment of problem (3.4) in cases of one and two spatial dimensions , that is, the reconstruction of the pair (Θ_0, Θ_1) for the problem (2.4).

For the Caputo fractional derivative of order (α), we discretize the time variable using the classical $L1$ scheme on a uniform grid with step size (Δt). At the time level (t_n), the Caputo derivative is approximated by

$$\partial_t^\alpha \Theta(x, t_n) \approx \frac{1}{\Gamma(2-\alpha)\Delta t^\alpha} \sum_{k=0}^{n-1} a_{n-k}, (\Theta(x, t_{k+1}) - \Theta(x, t_k)),$$

where the convolution weights are given by

$$a_j = (j+1)^{\cdot 1-\alpha} - j^{\cdot 1-\alpha}, \qquad j \geq 0.$$

The L^1 method delivers first-order accuracy in time for sufficiently smooth solutions, and retains key properties of the continuous problem, such as stability and monotonicity. Because of these features, it is widely used in numerical simulations of time-fractional diffusion and scattering models.

In our computations (see [7]), this L^1 approximation is coupled with a Nyström discretization for the spatial fractional Riesz Laplacian. The combination leads to a fully discrete system that, at each time level, reduces to solving a linear system for spatial degrees of freedom.

To simulate noise, a random perturbation is added to the data:

$$\Theta_{obs}^\varepsilon = \Theta_{obs} + \varepsilon\Theta_{obs}.(2.rand(size(\Theta_{obs}) - 1),$$

where $\varepsilon = \|\Theta_{obs}^\varepsilon - \Theta_{obs}\|_{L^2(\Omega)}$ specifies the equivalent noise level.

To evaluate the precision of the numerical solution produced by the proposed methods, we compute the error as follows:

$$e_i^k = \|\Theta_i^k - \Theta_i\|_{L^2(\Omega)}, \quad i = 0, 1.$$

Here, Θ_i represents the exact solution, while Θ_i^k denotes the initial conditions reconstructed in the k-th iteration.

The application also requires a stopping criterion. In our numerical experiments, defining criteria that apply to both synthetic and measured test data proved challenging. Since the changes in the

reconstruction of each iteration step became imperceptible in our case, the iterative process was monitored interactively and halted accordingly. Subsequently, the calculated relative error is expressed as follows:

$$Err(\Theta_i^k) = \frac{e_i^k}{\|\Theta_i\|}. \tag{5.1}$$

For the k-th iteration, the residual R_k takes the form

$$R_k = \|\Theta^k(x,T) - \Theta_{obs}\|_{L^2(\Omega)}. \tag{5.2}$$

Morozov's discrepancy principle is widely recognized as a leading method for this type of problem, and it relies on choosing the number of iterations k such that the inequality below is valid:

$$R_k \leq \tau\epsilon \leq R_{k-1}.$$

The constant ($\tau > 1$) is used as a leniency factor in the stopping criterion and is usually chosen with the value ($\tau = 1.01$).

5.1. One-dimensional case

Without loss of generality, the space domain is taken as $\Omega = [-1, 1]$, $T = 1$. In this case, the grid size for the time and space variable is fixed as $\Delta t = 1/200$ and $\Delta x = 1/200$, respectively, the order of the fractional time derivative α, and the order of the fractional Laplacian s are chosen as $\alpha = 1.5$, $s = 0.5$, respectively. To stabilize the inverse problem, the regularization parameter is fixed at a small value $\eta = 10^{-6}$ in all numerical tests.

In this case, we present two tests to show the effectiveness of the suggested methods. The results of the estimation of two initial values Θ_0, Θ_1 are provided for these Examples, which can be categorized into two types: regular Examples (Examples 5.1) and complex Examples (Examples 5.2).

Example 5.1. *In this experiment, our algorithm is used to reconstruct two unidentified initial values described as follows:*

$$\Theta_0(x) = (1-x^2)\left[\sin\left(\frac{\pi(x+1)}{2}\right) + \tfrac{1}{2}\cos\left(\frac{\pi(x+1)}{2}\right)\right], \Theta_1(x) = (1-x^2)\left[0.4 + 0.3\ \sin(\pi(x+1))\right],$$

from the final data measured $\Theta(.,T)$. The correspondence reconstruction results with various noise levels are shown in Figure 1.

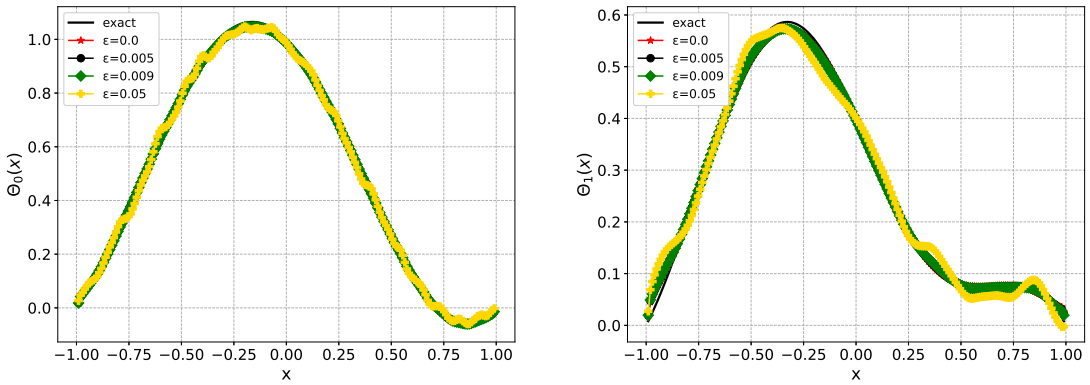

Figure 1. Reconstruction results for Example 5.1: (a) $\Theta_0(x)$ and (b) $\Theta_1(x)$.

Example 5.2. *In this specific case, we assess the performance of our algorithm in reconstructing unknown initial conditions that exhibit nonsmooth properties. The parameters* Θ_0 *and* Θ_1 *are determined using the measured final data and are defined as follows:*

$$\Theta_0(x) = (1 - x^2)\,\max(0,\, 1 - 1.2\,|x + 0.15|), \quad \Theta_1(x) = (1 - x^2)\chi_{[0.25,\,0.75]}(x).$$

The reference solution was calculated numerically using a very fine spatial and temporal discretization because the fractional Laplacian of the nonsmooth beginning condition in Example 5.2 is not available analytically. The precise profile for error assessment is then derived from this high-resolution solution.

From Figures 1 and 2, we can see that the numerical results for Examples 5.1 and 5.2 are quite accurate up to 5% noise added in the exact final data $\Theta(x, T)$. Moreover, one can deduce the following remarks:

- The numerical results of nonsmooth initial values Example 5.2 are less accurate compared to the numerical results of smooth functions Example 5.1.
- The efficiency and accuracy of our algorithm decrease with an increase in noise level.

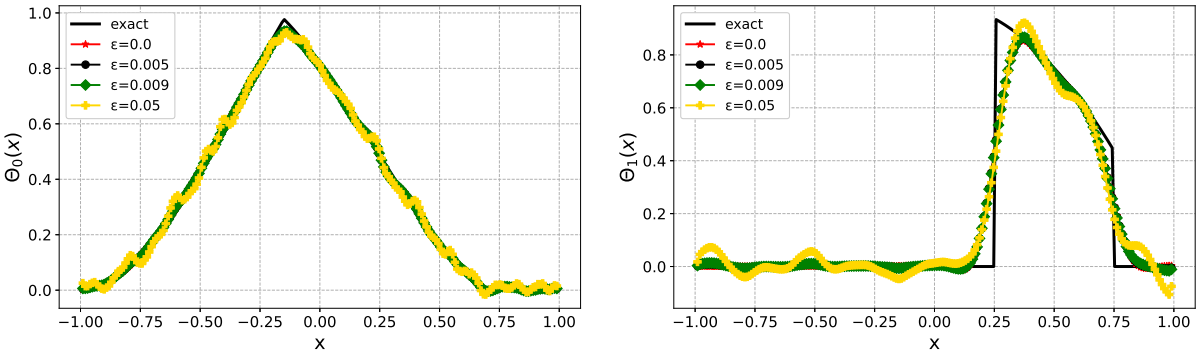

(a) **(b)**

Figure 2. Reconstruction results for Example 5.2: (a) $\Theta_0(x)$ and (b) $\Theta_1(x)$.

5.2. Convergence and stability results

This paragraph is concerned with the convergence and stability of the proposed algorithm. The approximation errors $(Err(\Theta_0, \Theta_1)$ for Example 5.1 with various noise levels are shown in Figure 3. It can be observed that the approximation errors become smaller as the noise levels decrease, after a few iterations, the computed errors have slightly increased, so we have to stop at a suitable step.

Figure 3 depicts the exponential decay of the relative errors $Err(\Theta_0(x))$, and $Err(\Theta_1(x))$, for a log-type function, which is steadily converging toward zero. The results indicate a clear trend of decreasing relative errors, highlighting exponential convergence. This behavior reflects the progressive improvement in accuracy with each iteration. The decreasing error values emphasize the efficiency of the estimation techniques in approximating the true initial values. These findings validate the robustness and reliability of the proposed methods, demonstrating their ability to accurately reconstruct $\Theta_0(x)$ and $\Theta_1(x)$,, through iterative refinement.

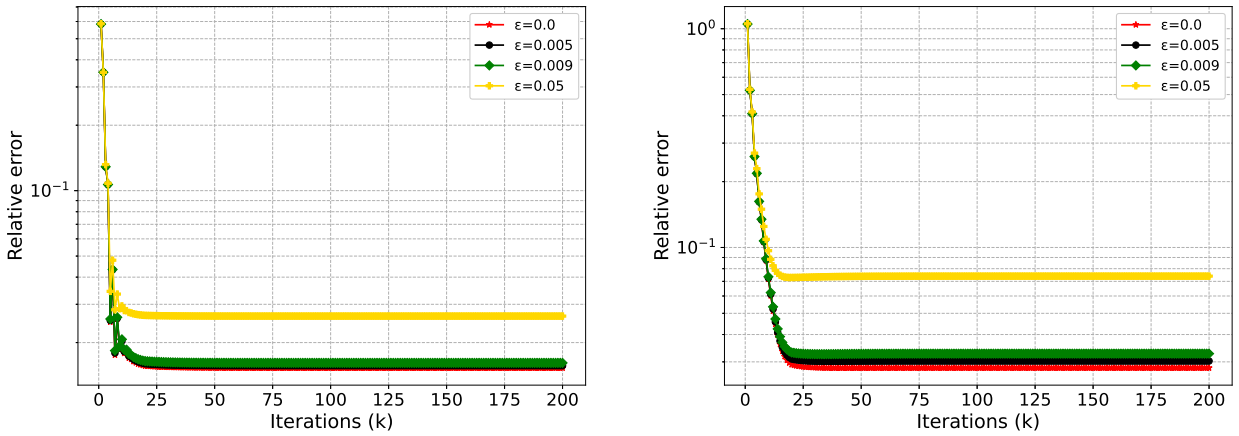

(a) **(b)**

Figure 3. Relative error for Example 5.2: (a) $Err(\Theta_0(x))$ and (b) $Err(\Theta_1(x))$.

Figure 4 shows that during the initial iterations, the residuals $R_k(\Theta_0)$ and $R_k(\Theta_1)$ show a rapid decrease, followed by a stabilizing phase at noise-dependent values. The Morozov discrepancy principle ensures the stability of the reconstructions and offers an automatic halting condition.

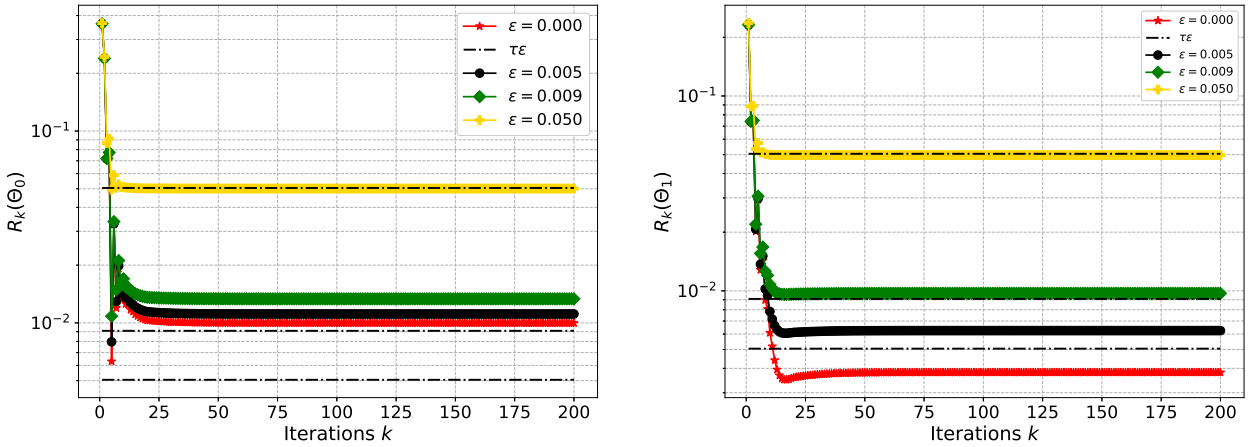

(a) **(b)**

Figure 4. The residual R_k for Example 5.2: (a) $R_k(\Theta_0(x))$ and (b) $R_k(\Theta_1(x))$.

5.3. Two-dimensional case

Now we proceed to the more challenging two-dimensional case, where we divide the space-time region $\Omega \times [0, T] := [-1, 1]^2 \times [0, 1]$ into $60 \times 60 \times 50$ equidistant meshes. Similarly to the one-dimensional examples, we will test the numerical performance of Algorithm 1 in the reconstruction of an example in the cases of $\eta = 10^{-6}, \alpha = 1.5$ and $s = 0.5$.

Algorithm 1 Conjugate gradient method.

1: **Initialization:** Choose $\Theta_0^0,\ \Theta_1^0$.

2: **Gradient computation:** Solve the direct and adjoint problems to obtain the gradients $\dfrac{\partial Q}{\partial \Theta_0^k}$ and $\dfrac{\partial Q}{\partial \Theta_1^k}$.

3: **Descent direction:** Update the directions $d_k^{(0)}$ and $d_k^{(1)}$.

4: **Step size:** Compute μ_k.

5: **Update:**

$$\Theta_0^{k+1} = \Theta_0^k + \mu_k d_k^{(0)},$$
$$\Theta_1^{k+1} = \Theta_1^k + \mu_k d_k^{(1)}.$$

6: Repeat until convergence.

Let us consider the following functions:

Example 5.3.

$$\Theta_0(x,y) = (1-x^2)(1-y^2)\sin\Big(\frac{\pi(x+1)}{2}\Big)\sin\Big(\frac{\pi(y+1)}{2}\Big),$$
$$\Theta_1(x,y) = (1-x^2)(1-y^2)\Big(0.5+0.3\cos\Big(\frac{\pi(x+1)}{2}\Big)\cos\Big(\frac{\pi(y+1)}{2}\Big)\Big).$$

The 3D surface of these functions is plotted in Figure 5.

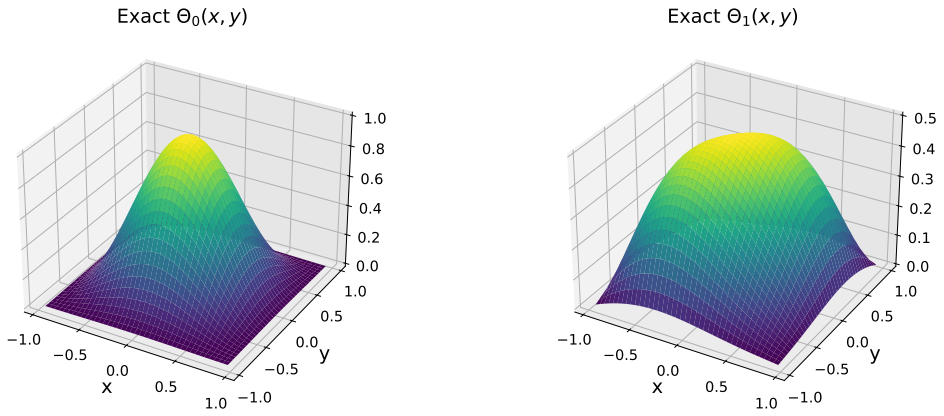

Figure 5. 3D surface of the Example 5.3.

The results in Figures 6 and 7 show that, in the absence of noise, the reconstructed solutions almost perfectly coincide with the true ones. When noise is added, the reconstructions gradually deviate from the exact solution, which is expected given the strong ill-posedness of the problem. However, the overall shape is still captured correctly. Together, these observations demonstrate that the proposed method performs well both in ideal conditions and at different noise levels.

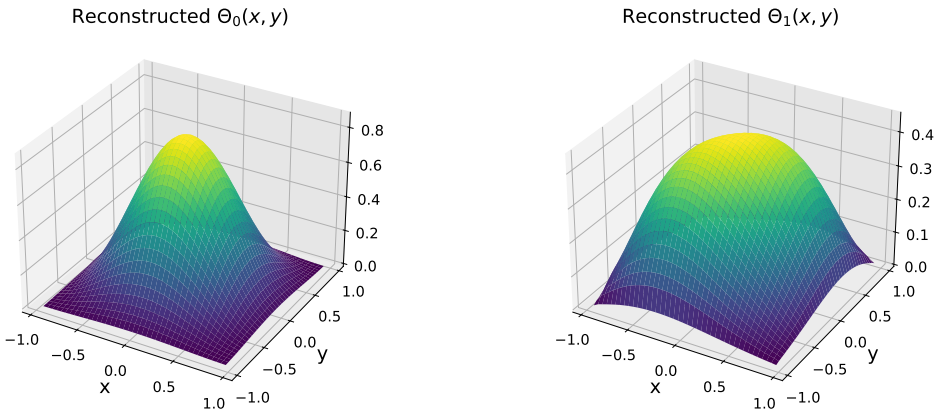

(a) **(b)**

Figure 6. The numerical results for Example 5.3 with $\epsilon = 0$.

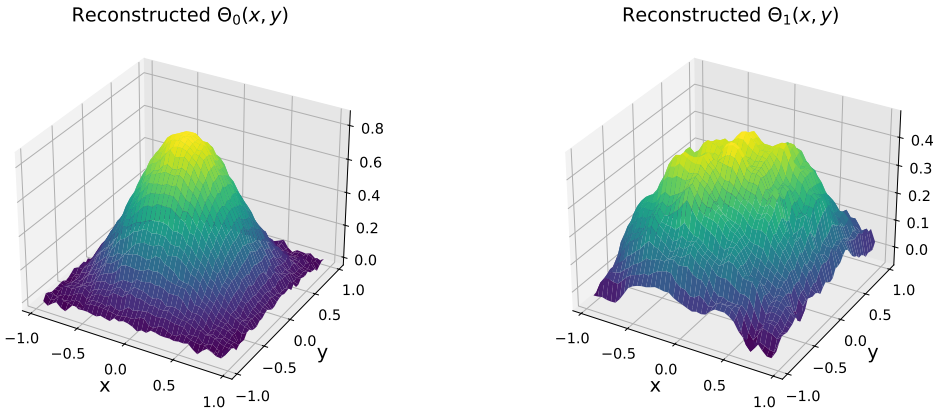

(a) **(b)**

Figure 7. The numerical results for Example 5.3 with $\epsilon = 0.05$.

Figures 8 and 9 clearly demonstrate the effect of noise. In the noise-free state (Figure 8), the error remains very small within the domain, and the contour lines appear smooth and regular, indicating that the reconstruction is very close to the true solution.

However, when noise is added at a rate of 0.05 *(Figure 9), the error increases and the contour lines become less regular, which is expected in such sensitive problems. Nevertheless, the error remains within an acceptable level and the overall shape of the solution is preserved, demonstrating that the method remains stable despite the presence of noise.*

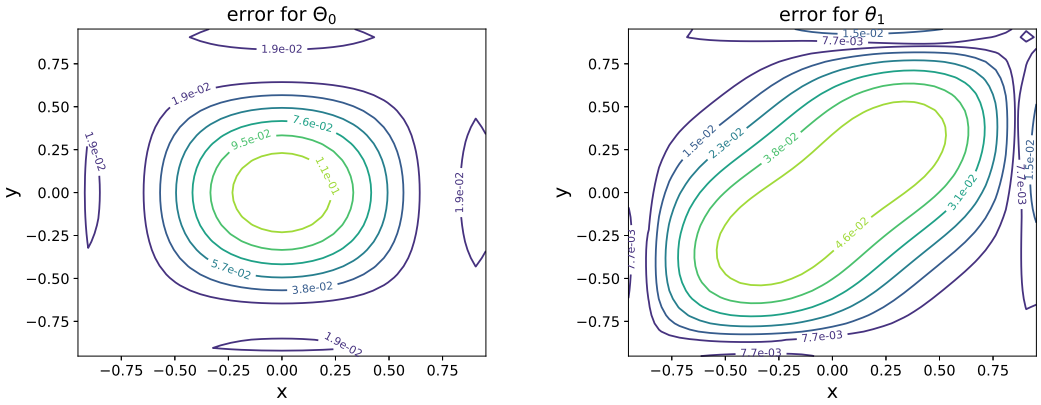

(a) **(b)**

Figure 8. Absolute error for Example 5.3 with $\epsilon = 0$.

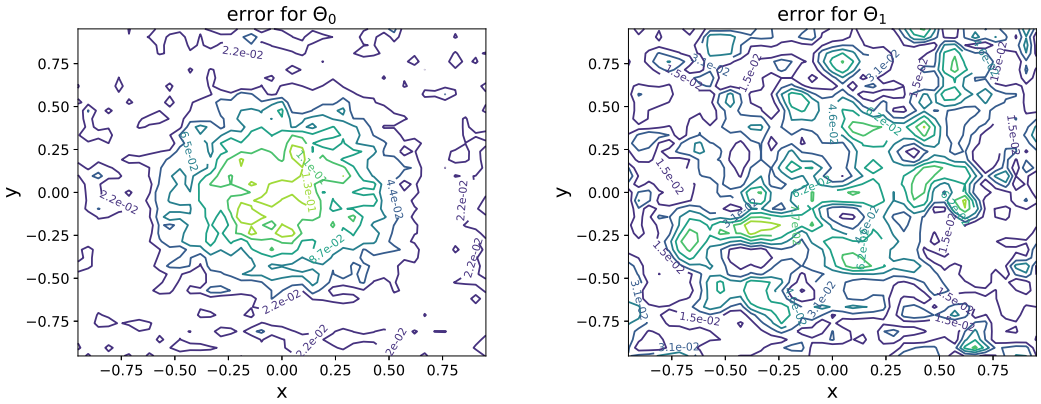

(a) **(b)**

Figure 9. Absolute error for Example 5.3 with $\epsilon = 0.05$.

6. Conclusions

This paper investigates an inverse problem related to a space-time fractional diffusion-wave equation, aiming to reconstruct two initial values from terminal time observations. First, we establish the validity of the forward problem by proving the existence and uniqueness of its solution. Since the corresponding inverse problem has a severely ill-posed problem, it is reformulated as a Tikhonov regularized problem, and the existence, uniqueness, and stability of the orderly solution are analyzed. The numerical solution of the resulting optimization problem is obtained using a conjugate gradient method.

A series of numerical experiments were conducted to evaluate the performance of the proposed approach by reconstructing several one-dimensional and two-dimensional test examples. The evolution of reconstruction errors and residuals was monitored during iterations. In particular, Morozov's variance principle was incorporated as a data-driven automatic stop criterion for the iterative ordering

process. The numerical results show that the proposed method produces accurate and stable reconstructions even in the presence of noise, confirming its effectiveness and robustness.

Although this study highlights several important theoretical and numerical results, some aspects still require further investigation in order to obtain a complete understanding of the problem. A detailed analysis of the convergence properties of the numerical scheme, its sensitivity to the regularization coefficient, and the influence of the initial conjecture remains essential. From a computational point of view, the extension of the current algorithm to larger or more distant domains is a promising prospect. In addition, the adaptation of the proposed method to more complex frameworks such as nonlinear problems or coupled systems of fractional partial differential equations represents a stimulating avenue of research for our future work.

Author contributions

Ghaziyah Alsahli, Mustapha Benoudi, Maawiya Ould Sidi, Eid Sayed Kamel, Ibrahim Omer Ahmed, MedYahya Ould-MedSalem and Hamed Ould Sidi: Conceptualization, Methodology, Validation, Writing-original draft, Writing-review & editing. All authors contributed equally to this work following CRediT.

Use of Generative-AI tools declaration

The authors declare they have not used Artificial Intelligence (AI) tools in the creation of this article.

Acknowledgment

This work was funded by the Deanship of Graduate Studies and Scientific Research at Jouf University under grant No. (DGSSR-2025-02-01116).

Conflicts of interest

The authors declare that they have no conflict of interest.

References

1. R. A. Adams, J. J. F. Fournier, *Sobolev spaces*, Amsterdam: Academic Press, 2003.
2. R. Almeida, A caputo fractional derivative of a function with respect to another function, *Commun. Nonlinear Sci.*, **44** (2017), 460–481. https://doi.org/10.1016/j.cnsns.2016.09.006
3. M. BenSaleh, H. Maatoug, Inverse source problem for a space-time fractional diffusion equation, *Ricerche Mat.*, **73** (2024), 681–713. https://doi.org/10.1007/s11587-021-00632-x
4. E. Di Nezza, G. Palatucci, E. Valdinoci, Hitchhiker's guide to the fractional sobolev spaces, *Bull. Sci. Math.*, **136** (2012), 521–573. https://doi.org/10.1016/j.bulsci.2011.12.004
5. K. Diethelm, N. J. Ford, Analysis of fractional differential equations, *J. Math. Anal. Appl.*, **265** (2002), 229–248. https://doi.org/10.1006/jmaa.2000.7194

6. S. Dipierro, X. Ros-Oton, E. Valdinoci, Nonlocal problems with neumann boundary conditions, *Rev. Mat. Iberoam.*, **33** (2017), 377–416. https://doi.org/10.4171/RMI/942
7. S. Duo, L. Ju, Y. Zhang, A fast algorithm for solving the space-time fractional diffusion equation, *Comput. Math. Appl.*, **75** (2018), 1929–1941. https://doi.org/10.1016/j.camwa.2017.04.008
8. Z. Fu, L. Yang, Q. Xi, C. Liu, A boundary collocation method for anomalous heat conduction analysis in functionally graded materials, *Comput. Math. Appl.*, **88** (2021), 91–109. https://doi.org/10.1016/j.camwa.2020.02.023
9. Z. Fu, L. Yang, H. Zhu, W. Xu, A semi-analytical collocation trefftz scheme for solving multi-term time fractional diffusion-wave equations, *Eng. Anal. Bound. Elem.*, **98** (2019), 137–146. https://doi.org/10.1016/j.enganabound.2018.09.017
10. J. W. He, Y. Liang, B. Ahmad, Y. Zhou, Nonlocal fractional evolution inclusions of order $\alpha \in (1, 2)$, *Mathematics*, **7** (2019), 209. https://doi.org/10.3390/math7020209
11. J. Janno, Y. Kian, Inverse source problem with a posteriori boundary measurement for fractional diffusion equations, *Math. Method. Appl. Sci.*, **46** (2023), 15868–15882. https://doi.org/10.1002/mma.9432
12. K. H. Karlsen, S. Ulusoy, Stability of entropy solutions for Lévy mixed hyperbolic-parabolic equations, arXiv: 0902.0538. https://doi.org/10.48550/arXiv.0902.0538
13. Y. Kian, Z. Li, Y. Liu, M. Yamamoto, The uniqueness of inverse problems for a fractional equation with a single measurement, *Math. Ann.*, **380** (2021), 1465–1495. https://doi.org/10.1007/s00208-020-02027-z
14. A. A. Kilbas, H. M. Srivastava, J. J. Trujillo, *Theory and applications of fractional differential equations*, Amsterdam: Elsevier Science, 2006.
15. M. M. Meerschaert, D. A. Benson, H. P. Scheffler, B. Baeumer, Stochastic solution of space-time fractional diffusion equations, *Phys. Rev. E*, **65** (2002), 041103. https://doi.org/10.1103/PhysRevE.65.041103
16. K. S. Miller, B. Ross, *An introduction to the fractional calculus and fractional differential equations*, Hoboken: Wiley, 1993.
17. V. A. Morozov, *Methods for solving incorrectly posed problems*, New York: Springer, 2012. https://doi.org/10.1007/978-1-4612-5280-1
18. D. A. Murio, Implicit finite difference approximation for time fractional diffusion equations, *Comput. Math. Appl.*, **56** (2008), 1138–1145. https://doi.org/10.1016/j.camwa.2008.02.015
19. K. Oldham, J. Spanier, *The fractional calculus theory and applications of differentiation and integration to arbitrary order*, New York: Academic Press, 1974.
20. H. O. Sidi, M. Huntul, M. O. Sidi, H. Emadifar, Identifying an unknown coefficient in the fractional parabolic differential equation, *Results in Applied Mathematics*, **19** (2023), 100386. https://doi.org/10.1016/j.rinam.2023.100386
21. H. O. Sidi, M. A. Zaky, W. Qiu, A. S. Hendy, Identification of an unknown spatial source function in a multidimensional hyperbolic partial differential equation with interior degeneracy, *Appl. Numer. Math.*, **192** (2023), 1–18. https://doi.org/10.1016/j.apnum.2023.05.021

22. F. Yang, J. Xu, X. Li, Simultaneous inversion of the source term and initial value of the time fractional diffusion equation, *Math. Model. Anal.*, **29** (2024), 193–214. https://doi.org/10.3846/mma.2024.18133

23. Y. Zhang, T. Wei, Y. X. Zhang, Simultaneous inversion of two initial values for a time-fractional diffusion-wave equation, *Numer. Meth. Part. Differ. Eq.*, **37** (2021), 24–43. https://doi.org/10.1002/num.22517

AIMS Press